

Velocity-space cascade in magnetized plasmas: Numerical simulations

O. Pezzi, S. Servidio, D. Perrone, F. Valentini, L. Sorriso-Valvo, A. Greco, W. H. Matthaeus, and P. Veltri

Citation: *Physics of Plasmas* **25**, 060704 (2018); doi: 10.1063/1.5027685

View online: <https://doi.org/10.1063/1.5027685>

View Table of Contents: <http://aip.scitation.org/toc/php/25/6>

Published by the [American Institute of Physics](#)

PHYSICS TODAY

WHITEPAPERS

MANAGER'S GUIDE

Accelerate R&D with
Multiphysics Simulation

READ NOW

PRESENTED BY

 **COMSOL**

Velocity-space cascade in magnetized plasmas: Numerical simulations

O. Pezzi,¹ S. Servidio,¹ D. Perrone,^{2,3} F. Valentini,¹ L. Sorriso-Valvo,⁴ A. Greco,¹ W. H. Matthaeus,⁵ and P. Veltri¹

¹Dipartimento di Fisica, Università della Calabria, Cosenza I-87036, Italy

²Department of Physics, Imperial College London, London SW7 2AZ, United Kingdom

³European Space Agency, ESAC, Madrid E-28692, Spain

⁴Nanotec-CNR, Sede di Rende, Rende I-87036, Italy

⁵Bartol Research Institute and Department of Physics and Astronomy, University of Delaware, Newark, Delaware 19716, USA

(Received 5 March 2018; accepted 11 June 2018; published online 26 June 2018)

Plasma turbulence is studied via direct numerical simulations in a two-dimensional spatial geometry. Using a hybrid Vlasov-Maxwell model, we investigate the possibility of a velocity-space cascade. A novel theory of space plasma turbulence has been recently proposed by Servidio *et al.* [Phys. Rev. Lett. **119**, 205101 (2017)], supported by a three-dimensional Hermite decomposition applied to spacecraft measurements, showing that velocity space fluctuations of the ion velocity distribution follow a broad-band, power-law Hermite spectrum $P(m)$, where m is the Hermite index. We numerically explore these mechanisms in a more magnetized regime. We find that (1) the plasma reveals spectral anisotropy in velocity space, due to the presence of an external magnetic field (analogous to spatial anisotropy of fluid and plasma turbulence); (2) the distribution of energy follows the prediction $P(m) \sim m^{-2}$, proposed in the above theoretical-observational work; and (3) the velocity-space activity is intermittent in space, being enhanced close to coherent structures such as the reconnecting current sheets produced by turbulence. These results may be relevant to the nonlinear dynamics weakly collisional plasma in a wide variety of circumstances. *Published by AIP Publishing.* <https://doi.org/10.1063/1.5027685>

Plasma turbulence is a challenging problem, involving a variety of complex nonlinear phenomena. In the classical picture of turbulence, both in ordinary fluids and collisional plasmas, whenever energy is injected into the system, a cross-scale transfer occurs, producing smaller scales and leading eventually to energy conversion and dissipation. This non-linear behavior transfers energy from macroscopic gradients into small plasma eddies, waves, and magnetic structures. The story becomes even more challenging in weakly collisional plasmas—systems far from local thermal (Maxwellian) equilibrium. The absence of an equilibrium attractor leaves the plasma state free to explore the dual spatial-velocity phase space.² This dynamics is responsible for strong deformations of the particle distribution function (DF), commonly classified as rings, beams, temperature anisotropy, velocity-space vortices, and so on.^{3–6} In this multi-dimensional space, energy can be transferred nonlinearly from physical space to velocity space (between waves and particles), and vice-versa, leading finally to the dissipation of the available energy through collisions.^{2,7–9,73}

The connection between turbulence and velocity-space deformations remains a great challenge for both theoretical and computational approaches. This scenario has been envisioned since the seminal works by Landau.¹⁰ Recently, the study of phase-space fluctuations has become a topic of renewed interest within the plasma community.^{11–14} Many important and useful suggestions on the possibility of a spatial-velocity cascade have been recently proposed, in the framework of reduced models of plasma turbulence such as drift-wave and gyrokinetics.^{15–18} These concepts, closely

related to strongly magnetized laboratory plasmas,¹⁹ need to be revised and further explored in the framework of space plasmas, where magnetic fluctuations are, very often, of the order of the mean magnetic field.²⁰ In these regimes, indeed, nonlinear Landau damping and ion-cyclotron resonances, as well as interactions with current layers and zero-frequency structures, might occur in a more complex way.^{21,22}

In the last decade or so, Vlasov-based simulations have been extensively used to investigate the complexity of plasma turbulence.^{23–34} Numerical experiments suggest a strong connection between turbulence and non-Maxwellian features in the particle DF.^{35–38} Recently, the unprecedented-resolution and high-accuracy of measurements from the Magnetospheric Multiscale Mission (MMS)⁶ have enabled direct observation of the velocity space cascade in a space plasmas.¹ In particular, a three-dimensional (3D) Hermite decomposition has been applied to spacecraft measurements, showing that the ion velocity distribution has a broad-band Hermite spectrum $P(m)$, where m is an Hermite mode index (see below). A Kolmogorov-like phenomenology has been proposed to interpret the observations, suggesting two types of phase-space cascade: (1) the isotropic cascade, with $P(m) \sim m^{-3/2}$, when the plasma is weakly magnetized (such as in the terrestrial, shocked magnetosheath) and (2) $P(m) \sim m^{-2}$, for more highly magnetized cases. Here, we inspect the latter situations, exploring the possibility of an anisotropic cascade in velocity space, establishing its relation with spatial intermittency.

In this Letter, we employ a Hermite decomposition to analyze a hybrid Vlasov-Maxwell (HVM) simulation^{39,40} of

collisionless plasma dynamics. Noise-free HVM simulations are well-suited for the study of the kinetic effects in turbulent collisionless plasmas. We integrate the dimensionless HVM equations written as

$$\frac{\partial f}{\partial t} + \mathbf{v} \cdot \frac{\partial f}{\partial \mathbf{x}} + (\mathbf{E} + \mathbf{v} \times \mathbf{B}) \cdot \frac{\partial f}{\partial \mathbf{v}} = 0, \quad (1)$$

$$\frac{\partial \mathbf{B}}{\partial t} = -\nabla \times \mathbf{E} = \nabla \times \left[\mathbf{u} \times \mathbf{B} - \frac{\mathbf{j} \times \mathbf{B}}{n} + \frac{\nabla P_e}{n} - \eta \mathbf{j} \right], \quad (2)$$

where $f(\mathbf{x}, \mathbf{v}, t)$ is the proton DF, and \mathbf{E} and \mathbf{B} are the electric and magnetic fields, respectively. The current density is $\mathbf{j} = \nabla \times \mathbf{B}$, n and \mathbf{u} represent the first two moments of f , and P_e is the isothermal pressure of the massless fluid electrons. In the above equations, time, velocities, and lengths are scaled to the inverse proton cyclotron frequency $\Omega_{cp}^{-1} = m_p c / e B_0$, to the Alfvén speed $c_A = B_0 / \sqrt{4\pi n_0 m_p}$, and to the proton skin depth $d_p = c_A / \Omega_{cp}$, respectively, where m_p , e , c , B_0 , and n_0 the proton mass, charge, the light speed, the background magnetic field, and the equilibrium proton density. A small resistivity $\eta = 2 \times 10^{-2}$, judiciously selected to have a slight influence on the evolution of the power spectra, suppresses spatial numerical instabilities at wavenumber larger than $kd_p \simeq 10$.⁴⁰ For the velocity space, the Eulerian scheme adopted in the algorithm introduces a small diffusion. The effects of this artificial dissipation are however almost negligible, violating conservation of entropy up to 0.1%.

Equations (1) and (2) are integrated in a 2.5D-3 V phase space domain, i.e., all velocity space directions are retained while, in physical space, all vector components are retained but they depend only on the two spatial coordinates (x, y) . We discretized the double-periodic spatial domain of size $L = 2\pi \times 20d_p$, with $N_x = N_y = 512$ grid-points in each direction. The velocity domain is discretized by $N_{v_x} = N_{v_y} = N_{v_z} = 71$ points in the range $v_j = [-5v_{th}, 5v_{th}]$ ($j = x, y, z$) and boundary conditions impose $f(v_j > 5v_{th}) = 0$, $v_{th} = \sqrt{k_B T_0 / m_p}$ being the proton thermal speed, related to the Alfvén speed through $\beta = 2v_{th}^2 / c_A^2 = 0.5$. Further details on the numerics can be found in Refs. 41 and 42. The proton DF is initially Maxwellian, with uniform unit density. In order to explore the possibility of a magnetized phase-space cascade, a uniform background out-of-plane magnetic field $\mathbf{B}_0 = B_0 \mathbf{e}_z$ ($B_0 = 1$) is also imposed. The equilibrium is then perturbed through a 2D spectrum of Fourier modes, as described in Servidio *et al.*⁴⁰ The r.m.s. level of magnetic fluctuations is $\delta B / B_0 = 1/3$, corresponding to typical conditions for a solar-wind like plasma. These parameters are significantly different from the MMS observations studied in Servidio *et al.*,¹ where $\delta B / B_0 \sim 2$ and $\beta \gg 1$, indicating a weakly magnetized magnetosheath plasma. Such differences may significantly influence the velocity space cascade, as discussed below.

We will discuss the results at the peak of the nonlinear activity, namely, at $t^* = 49\Omega_{cp}^{-1}$, where $\langle j_z^2 \rangle$ reaches its maximum. To characterize the presence of small-scale fluctuations, the left panel of Fig. 1 reports the omni-directional perpendicular power spectral density of magnetic field (black), proton bulk speed (blue), electric field (green

dotted), and proton density (red dashed), as a function of kd_p . The red dotted line indicates, as a reference, the Kolmogorov exponent $-5/3$. Magnetic fluctuations dominate at the large scales and the inertial range, while at smaller kinetic scales electric field spectral power is higher.^{43,44} Moreover, although the large scales are essentially incompressible, at kinetic scales the compressibility increases.⁴⁵

Strong current sheets are evident in the shaded-contour of Fig. 1 (central panel), which shows the out-of-plane current density $|j_z(x, y)|$ at $t = t^*$. As expected in turbulence, local narrow current layers develop and become important sites of reconnection and dissipation.^{40,46-48} Previous works have suggested that these intermittent regions are related to interesting non-Maxwellian features of the DF,³⁵ a very well known property of magnetic reconnection.⁴⁹⁻⁵¹ A simple non-Maxwellianity indicator,^{35,52} measuring deviations of the particle DF from the corresponding Maxwellian g , has been defined as

$$\epsilon(\mathbf{x}) = \frac{1}{n} \sqrt{\int (f - g)^2 d^3v}. \quad (3)$$

The right panel of Fig. 1 shows $\epsilon(x, y)$ at $t = t^*$, suggesting that the non-fluid activity is highly intermittent, correlated with the most intense current sheets. The scalar function ϵ quantifies the presence of high-order moments of the plasma, and includes moments of the proton DF, such as temperature anisotropy, heat flux, kurtosis, and so on. It does not reveal, however, the particular structure of the velocity subspace.

In order to quantify details of the phase-space cascade, we will adopt a 3D Hermite transform representation of $f(\mathbf{x}, \mathbf{v})$, a valuable tool for plasma theory.⁵³⁻⁵⁵ A 1D basis can be defined as

$$\psi_m(v) = \frac{H_m\left(\frac{v-u}{v_{th}}\right)}{\sqrt{2^m m!} \sqrt{\pi} v_{th}} e^{-\frac{(v-u)^2}{2v_{th}^2}}, \quad (4)$$

where u and v_{th} are now the local bulk and thermal speed, respectively, and $m \geq 0$ is an integer (we simplified the notation suppressing the spatial dependence). The eigenfunctions obey the orthogonality condition $\int_{-\infty}^{\infty} \psi_m(v) \psi_l(v) dv = \delta_{ml}$. Using this basis, one obtains a 3D representation of the distribution function $f(\mathbf{v}) = \sum_{\mathbf{m}} f_{\mathbf{m}} \psi_{\mathbf{m}}(\mathbf{v})$. The above projection quantifies high-order corrections to the particle velocity DF, since the basis is shifted in the local fluid velocity frame, normalized to the ambient density and temperature. The projection in Eq. (4) is equivalent to shifting the Hermite grid in the local plasma frame, renormalizing such that the temperature is unity. Missing the above shift would generate a convolution with the central Maxwellian kernel and therefore a misleading spectrum. A Gauss-Hermite quadrature is adopted,^{1,56} for efficiency, and to avoid spurious aliasing and convergence problems. As described in Servidio *et al.*,¹ we interpolate the distribution function at the Gaussian quadrature knots, using a second order interpolation. We tested the

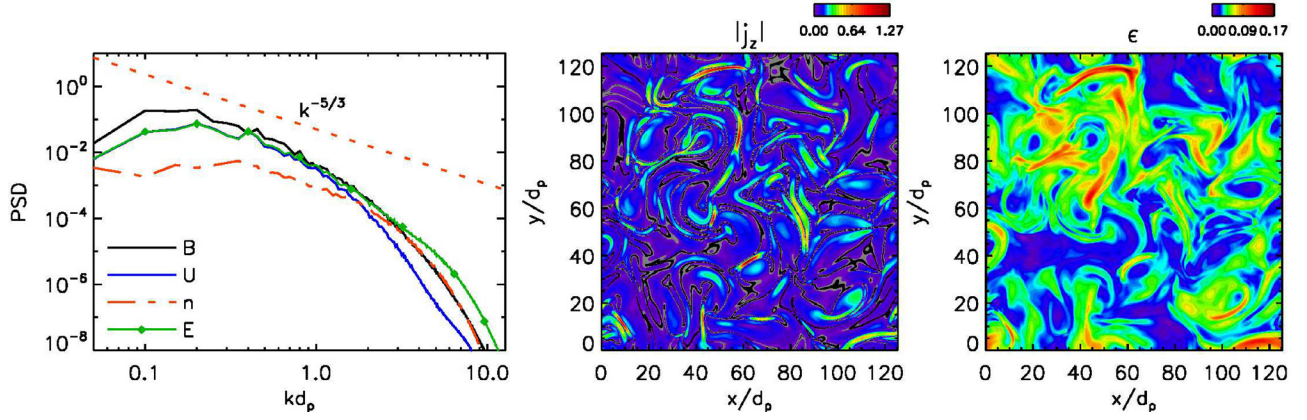


FIG. 1. Overview of the numerical results at the peak of the nonlinear activity, $t^* = 49\Omega_{cp}^{-1}$. Left: omnidirectional perpendicular spectra of magnetic field B (black), proton bulk speed U (blue), electric field E (green dotted), and proton density n (red dashed), in code units. Center: contour plot of the current density $|j_z|$. Right: map of the non-Maxwellianity function ϵ , as defined in the text.

accuracy of our Hermite transform, verifying that the Parseval-Plancercel spectral theorem is satisfied up to the machine precision.

Using the above procedure, the Hermite coefficients $f_m = \int_{-\infty}^{\infty} f(\mathbf{v})\psi_m(\mathbf{v})d^3v$ have been computed. Note that the Hermite projection has a profound meaning for gases, since the index m roughly corresponds to an order of the velocity moments:¹⁸ the $m=1$ coefficient corresponds to bulk flow fluctuations; $m=2$ corresponds to temperature deformations; $m=3$ to heat flux perturbations; and so on. Finally, it is worth noting that a highly deformed $f(\mathbf{v})$ would produce plasma enstrophy,⁵⁷ defined as

$$\Omega(\mathbf{x}) \equiv \int_{-\infty}^{\infty} \delta f^2(\mathbf{x}, \mathbf{v})d^3v = \sum_{m>0} [f_m(\mathbf{x})]^2, \quad (5)$$

where δf indicates the difference from the ambient Maxwellian, as in Eq. (3). It is interesting to note that the latter quantity is related to the Maxwellianity indicator ϵ , $\Omega = \epsilon^2 n^2$, and is essentially the free energy in gyrokinetics.¹⁸

In the Hermite transform, we set $N_m = 100$ modes in each velocity direction, applying the projection to a subset of the original volume. In particular, we choose equally spaced spatial points on a grid that is coarser than the original 512×512 , to reduce computational efforts (although the algorithm uses MPI parallel architecture). We have checked that statistical convergence is attained for an ensemble of 32×32 proton velocity DFs (not shown). In our analysis, we ensure convergence by using an ensemble of 64×64 velocity DFs. From the coefficients $f_m(\mathbf{x}) \equiv f_m(x, y, m_x, m_y, m_z)$, we define the enstrophy spectra as $P(m_x, m_y, m_z) = \langle f_m(\mathbf{x})^2 \rangle$, where $\langle \dots \rangle$ indicates spatial average. Note that details of the phase space structure are lost when the Hermite spectrum is computed for poorly resolved data, or when the spectrum is reduced (integrated over a velocity coordinate).

The 2D enstrophy spectrum is evaluated by reducing $P(m_x, m_y, m_z)$ in different directions, as, for example, $P(m_x, m_y) = \sum_{m_z=0}^{N_m} P(m_x, m_y, m_z)$. Figure 2 reports the 2D reduced spectra $P(m_x, m_y)$ (a) and $P(m_x, m_z)$ (b). The enstrophy is fairly isotropic in the plane (m_x, m_y) , perpendicular to the background magnetic field. On the other hand, an

anisotropy is revealed when considering the direction of B_0 , namely, the m_z axis: spectra are stretched in the parallel direction. This might indicate the presence of structures along the background field and the presence of Landau resonances.⁵⁸ Such anisotropy is analogous to the spatial anisotropy commonly observed in plasmas, when a strong imposed magnetic field is present.⁵⁹ However, in contrast to what is observed in the physical space, velocity gradients are stronger along the mean field, while the cascade is inhibited across it. This may be compatible with the presence of structures in the distribution functions, such as rings and beams of trapped particles, commonly recovered along the ambient magnetic field. The plasma β may also significantly affect velocity space anisotropy. For example, β controls the possible interactions between the particles in the core of the VDF and waves,^{60–64} and consequently the generation of structures along the background magnetic field. It should be noted that the velocity-space anisotropy present in our simulation was not observed in the magnetosheath observations of MMS,¹ where both the plasma β and the magnetic fluctuations $\delta B/B_0$ were significantly larger.

We evaluated the isotropic (omnidirectional) 1D Hermite spectra, by summing $P(m_x, m_y, m_z)$ over concentric shells of unit width, i.e., $P(m) = \sum_{m-\frac{1}{2} < m' \leq m+\frac{1}{2}} P(m')$. Figure 3(a) shows the isotropic Hermite spectrum $P(m)/P(0)$ at $t = t^* = 49\Omega_{cp}^{-1}$ (we normalized the spectrum to the mode $m=0$, which is the Maxwellian profile). The spectrum shows a power-law behavior for the first decade, indicating the presence

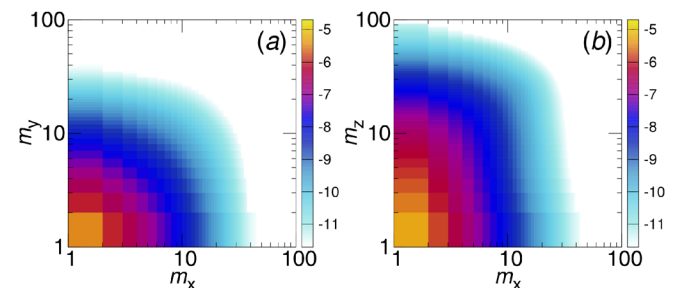


FIG. 2. Two-dimensional, reduced Hermite spectra, averaged over space. Panel (a) represents $P(m_x, m_y)$ (integrated over m_z), while (b) includes the anisotropy direction of the mean magnetic field B_0 .

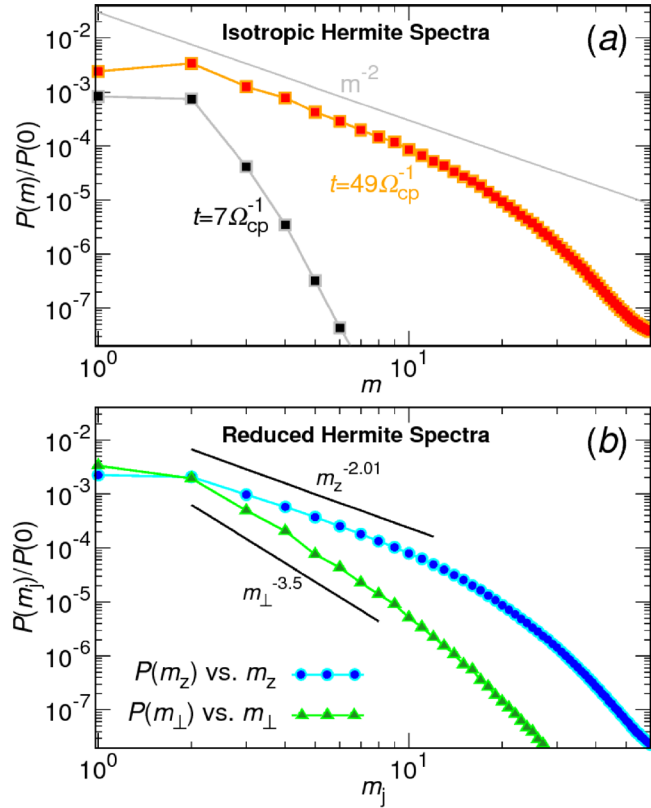


FIG. 3. (a) Isotropic Hermite power spectrum, at two times of the simulation. The prediction for the magnetized case is reported as a reference. (b) Reduced spectra along and across the mean field, at $t = 49\Omega_{cp}^{-1}$. The power-law fit in the parallel direction is consistent with the prediction $\sim m_z^{-2}$.

of phase-space cascade-like processes.^{1,11,12,17,18,65–68} The Hermite analysis on the HVM simulations shows a spectral break around $m \simeq 15$, where the artificial dissipation of the Eulerian scheme might affect the dynamics. In the same panel (a), we also plot the energy at an earlier time of the simulation, showing that the cascade has progressively emerged, as it would in physical space, by gradually filling in modes towards higher m -values, therefore creating finer velocity-space structures. In Fig. 3(b), we show the reduced spectra along the mean magnetic field (integrated over m_x and m_y), and the isotropic perpendicular spectrum $P(m_{\perp})$ (integrated over m_z and over concentric perpendicular shells m_{\perp}). While $P(m_z)$ is consistent with the m^{-2} phenomenological model, the reduced perpendicular spectrum $P(m_{\perp})$ is much lower in energy and is steeper, with exponent close to -3.5 . The significance of such anisotropy of the Hermite spectra will be investigated more in detail in future works. The results presented here differ from the ones of Ref. 14, in part, due to the different velocity space resolution adopted in the two papers. Here, we increased the velocity resolution, a feature crucial to properly describe the velocity space cascade. For maintaining an affordable computational cost, we chose a 2.5D physical space. Evidently, reducing from a 3D to a 2.5D physical space does not represent a strong limitation in describing statistical plasma dynamics at ion kinetic scales.^{28,69–71} On the other hand, Cerri, Kunz, and Califano¹⁴ performed a 3D–3V simulation but they have been forced to set a reduced velocity space resolution for decreasing the global computational cost of the simulation. Technical differences in

the implementation of the Hermite transform may also lead to the observed discrepancies.

In analogy with intermittency in turbulence, it is natural to ask whether or not the enstrophy transfer is homogeneous in space, as suggested by Fig. 1 (center and right panels). To this aim, we define the *Hermite spectrogram* $P(x, m)$, the isotropic Hermite spectrum as a function of the position. This tool might be also useful for spacecraft measurements. Figure 4(a) shows $P(x, m)$ along a one-dimensional spatial cut. The dual-space cascade is clearly intermittent: the spectrum amplitude and exponent depend on the position, with regions of low activity being interrupted by bursts of velocity-space activity. Only the ensemble average converges to the theoretical predictions represented in Fig. 3. In panel (b), we show a spatial cut of the current density $|j_z|$ (red) and of the plasma enstrophy Ω (blue), suggesting that the velocity space cascade is correlated with the intermittent current structures.

Motivated by recent theories and observations,^{1,72} we have studied plasma turbulence via direct numerical simulations, in a simplified 2.5D–3V geometry. Using a hybrid Vlasov–Maxwell model, we observed that the proton velocity distribution function produces broad-band fluctuations in the v -space. By using a 3D Hermite decomposition, we observed power-law Hermite spectra $P(m)$, indicative of a *velocity inertial range*. This velocity cascade establishes as the turbulence develops, resembling a mode-by-mode transfer, similar to the Kolmogorov phenomenology. Exploring a moderately magnetized case ($\delta B/B_0 \sim 1/3$ and $\beta = 0.5$) we found that: (1) the Hermite spectrum is shallower along the ambient magnetic field, indicating spectral anisotropy in the velocity space. This may be due to the mean magnetic field⁵⁹ and to the small plasma β ,^{60,61} which may generate structures in the parallel direction. (2) The distribution of energy follows the prediction $P(m) \sim m^{-2}$, and a much steeper exponent in the perpendicular direction, where $P(m_{\perp}) \sim m_{\perp}^{-3.5}$. Finally, (3) the velocity space activity is intermittent in real space, and is enhanced close to coherent structures such as the

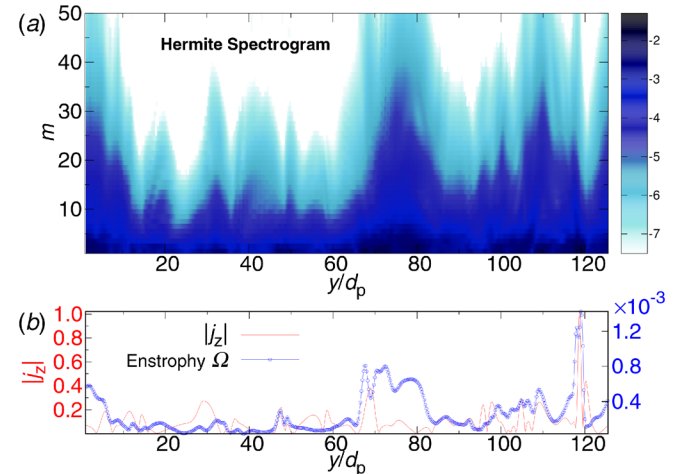


FIG. 4. (a) Hermite spectrogram, along a 1D cut through the simulation box, at $x^* \sim 50d_p$. The velocity space activity is highly intermittent. (b) Spatial profile at x^* of the current density $|j_z|$, together with the plasma enstrophy defined by Eq. (5). The velocity space cascade is correlated with intermittent coherent structures.

reconnecting current layers produced by turbulence. In future works, we plan to explore different plasma regimes, as well as the role played by the dimensionality of the system and by the electron kinetics. These results may be of fundamental significance as the space and astrophysical plasma communities move towards more complete understanding of the mechanisms leading to dissipation and heating in turbulent plasmas.

This research was partially supported by AGS-1460130 (SHINE), NASA Grant Nos. NNX14AI63G (Heliophysics Grand Challenge Theory), NNX15AB88G, and NNX17AB79G, the Solar Probe Plus Science Team (ISOIS/Princeton subcontract SUB0000165), and by the MMS Theory and Modeling team, No. NNX14AC39G. F.V. and O.P. are supported by Agenzia Spaziale Italiana under Contract No. ASI-INAF 2015-039-R.O. D.P., S.S., and L.S.V. acknowledge support from the Faculty of the European Space Astronomy Centre (ESAC). Numerical simulations discussed here have been performed on the Newton cluster at the University of Calabria. This work was partly supported by the International Space Science Institute (ISSI) in the framework of the International Team 405 entitled “Current Sheets, Turbulence, Structures and Particle Acceleration in the Heliosphere.” The authors would like to thank the anonymous reviewers for their suggestions, which significantly improved the quality of the paper.

- ¹S. Servidio, A. Chasapis, W. H. Matthaeus, D. Perrone, F. Valentini, T. N. Parashar, P. Veltri, D. Gershman, C. T. Russell, B. Giles, S. A. Fuselier, T. D. Phan, and J. Burch, *Phys. Rev. Lett.* **119**, 205101 (2017).
- ²K. Huang, *Statistical Mechanics* (Wiley, New York, 1963).
- ³N. A. Krall and A. W. Trivelpiece, *Principle Plasma Physics* (McGraw-Hill, New York, 1973).
- ⁴E. Marsch, K.-H. Mühlhäuser, R. Schwenn, H. Rosenbauer, W. Pilipp, and F. Neubauer, *J. Geophys. Res.: Space Phys.* **87**, 52, <https://doi.org/10.1029/JA087iA01p00052> (1982).
- ⁵P. Hellinger, P. Trávníček, J. C. Kasper, and A. J. Lazarus, *Geophys. Res. Lett.* **33**, L09101, <https://doi.org/10.1029/2006GL025925> (2006).
- ⁶J. L. Burch, T. E. Moore, R. B. Torbert, and B. L. Giles, *Space Sci. Rev.* **199**, 5 (2016).
- ⁷A. B. Mikhailovskii, “Theory of plasma instabilities,” in *Instabilities in an Inhomogeneous Plasma* (Plenum, New York, 1974), Vol. 2.
- ⁸O. Pezzi, F. Valentini, and P. Veltri, *Phys. Rev. Lett.* **116**, 145001 (2016).
- ⁹G. G. Howes, *Phys. Plasmas* **25**, 055501 (2018).
- ¹⁰L. Landau, *Zh. Eksp. Teor. Fiz.* **16**, 574 (1946), available at <http://cds.cern.ch/record/437300>.
- ¹¹T. Tatsuno, W. Dorland, A. A. Schekochihin, G. G. Plunk, M. Barnes, S. C. Cowley, and G. G. Howes, *Phys. Rev. Lett.* **103**, 015003 (2009); e-print [arXiv:0811.2538](https://arxiv.org/abs/0811.2538) [physics.plasm-ph].
- ¹²J. T. Parker, E. G. Highcock, A. A. Schekochihin, and P. J. Dellar, *Phys. Plasmas* **23**, 070703 (2016).
- ¹³J. M. TenBarge and G. G. Howes, *Astrophys. J. Lett.* **771**, L27 (2013); e-print [arXiv:1304.2958](https://arxiv.org/abs/1304.2958) [physics.plasm-ph].
- ¹⁴S. S. Cerri, M. W. Kunz, and F. Califano, *Astrophys. J. Lett.* **856**, L13 (2018); e-print [arXiv:1802.06133](https://arxiv.org/abs/1802.06133) [physics.plasm-ph].
- ¹⁵T. H. Watanabe and H. Sugama, *Phys. Plasmas* **11**, 1476 (2004).
- ¹⁶D. R. Hatch, F. Jenko, A. B. Navarro, and V. Bratanov, *Phys. Rev. Lett.* **111**, 175001 (2013).
- ¹⁷A. Kanekar, A. A. Schekochihin, W. Dorland, and N. F. Loureiro, *J. Plasma Phys.* **81**, 305810104 (2015); e-print [arXiv:1403.6257](https://arxiv.org/abs/1403.6257) [physics.plasm-ph].
- ¹⁸A. A. Schekochihin, J. T. Parker, E. G. Highcock, P. J. Dellar, W. Dorland, and G. W. Hammett, *J. Plasma Phys.* **82**, 905820212 (2016); e-print [arXiv:1508.05988](https://arxiv.org/abs/1508.05988) [physics.plasm-ph].
- ¹⁹P. G. Eltgroth, *Phys. Fluids* **17**, 1602 (1974).
- ²⁰M. L. Goldstein, D. A. Roberts, and W. H. Matthaeus, *Ann. Rev. Astron. Astrophys.* **33**, 283 (1995).
- ²¹G. G. Howes, K. G. Klein, and T. C. Li, *J. Plasma Phys.* **83**, 705830102 (2017).
- ²²O. Pezzi, F. Malara, S. Servidio, F. Valentini, T. N. Parashar, W. H. Matthaeus, and P. Veltri, *Phys. Rev. E* **96**, 023201 (2017).
- ²³G. G. Howes, S. C. Cowley, W. Dorland, G. W. Hammett, E. Quataert, and A. A. Schekochihin, *J. Geophys. Res.* **113**, A05103, <https://doi.org/10.1029/2007JA012665> (2008).
- ²⁴T. N. Parashar, M. A. Shay, P. A. Cassak, and W. H. Matthaeus, *Phys. Plasmas* **16**, 032310 (2009).
- ²⁵F. Valentini, D. Perrone, and P. Veltri, *Astrophys. J.* **739**, 54 (2011).
- ²⁶W. H. Matthaeus, S. Oughton, K. T. Osman, S. Servidio, M. Wan, S. P. Gary, M. A. Shay, F. Valentini, V. Roytershteyn, H. Karimabadi, and S. C. Chapman, *Astrophys. J.* **790**, 155 (2014).
- ²⁷S. Servidio, F. Valentini, F. Califano, and P. Veltri, *Phys. Rev. Lett.* **108**, 045001 (2012).
- ²⁸M. Wan, W. H. Matthaeus, V. Roytershteyn, H. Karimabadi, T. Parashar, P. Wu, and M. Shay, *Phys. Rev. Lett.* **114**, 175002 (2015).
- ²⁹F. Valentini, C. L. Vásconez, O. Pezzi, S. Servidio, F. Malara, and F. Pucci, *Astron. Astrophys.* **599**, A8 (2017).
- ³⁰O. Pezzi, T. N. Parashar, S. Servidio, F. Valentini, C. L. Vásconez, Y. Yang, F. Malara, W. H. Matthaeus, and P. Veltri, *Astrophys. J.* **834**, 166 (2017).
- ³¹S. Servidio, C. T. Haynes, W. H. Matthaeus, D. Burgess, V. Carbone, and P. Veltri, *Phys. Rev. Lett.* **117**, 095101 (2016); e-print [arXiv:1608.01207](https://arxiv.org/abs/1608.01207) [physics.plasm-ph].
- ³²L. Franci, S. Landi, L. Matteini, A. Verdini, and P. Hellinger, *Astrophys. J.* **812**, 21 (2015); e-print [arXiv:1506.05999](https://arxiv.org/abs/1506.05999) [astro-ph.SR].
- ³³L. Franci, A. Verdini, L. Matteini, S. Landi, and P. Hellinger, *Astrophys. J. Lett.* **804**, L39 (2015); e-print [arXiv:1503.05457](https://arxiv.org/abs/1503.05457) [astro-ph.SR].
- ³⁴P. Hellinger, L. Matteini, S. Landi, A. Verdini, L. Franci, and P. Trávníček, *Astrophys. J. Lett.* **811**, L32 (2015); e-print [arXiv:1508.03159](https://arxiv.org/abs/1508.03159) [physics.plasm-ph].
- ³⁵A. Greco, F. Valentini, S. Servidio, and W. Matthaeus, *Phys. Rev. E* **86**, 066405 (2012).
- ³⁶A. Chasapis, W. H. Matthaeus, T. N. Parashar, O. LeContel, A. Retinò, H. Breuillard, Y. Khotyaintsev, A. Vaivads, B. Lavraud, E. Eriksson, T. E. Moore, J. L. Burch, R. B. Torbert, P.-A. Lindqvist, R. E. Ergun, G. Marklund, K. A. Goodrich, F. D. Wilder, M. Chutter, J. Needell, D. Rau, I. Dors, C. T. Russell, G. Le, W. Magnes, R. J. Strangeway, K. R. Bromund, H. K. Leinweber, F. Plaschke, D. Fischer, B. J. Anderson, C. J. Pollock, B. L. Giles, W. R. Paterson, J. Dorelli, D. J. Gershman, L. Avanov, and Y. Saito, *Astrophys. J.* **836**, 247 (2017).
- ³⁷L. Sorriso-Valvo, D. Perrone, O. Pezzi, F. Valentini, S. Servidio, Y. Zouganelis, and P. Veltri, *J. Plasma Phys.* **84**, 725840201 (2018).
- ³⁸L. Sorriso-Valvo, F. Carbone, S. Perri, A. Greco, R. Marino, and R. Bruno, *Sol. Phys.* **293**, 10 (2018).
- ³⁹F. Valentini, S. Servidio, D. Perrone, F. Califano, W. Matthaeus, and P. Veltri, *Phys. Plasmas* **21**, 082307 (2014).
- ⁴⁰S. Servidio, F. Valentini, D. Perrone, A. Greco, F. Califano, W. H. Matthaeus, and P. Veltri, *J. Plasma Phys.* **81**, 325810107 (2015).
- ⁴¹F. Valentini, P. Trávníček, F. Califano, P. Hellinger, and A. Mangeney, *J. Comput. Phys.* **225**, 753 (2007).
- ⁴²D. Perrone, F. Valentini, and P. Veltri, *Astrophys. J.* **741**, 43 (2011).
- ⁴³S. D. Bale, P. J. Kellogg, F. S. Mozer, T. S. Horbury, and H. Reme, *Phys. Rev. Lett.* **94**, 215002 (2005).
- ⁴⁴L. Matteini, O. Alexandrova, C. H. K. Chen, and C. Lacombe, *Mon. Not. R. Astron. Soc.* **466**, 945–951 (2017).
- ⁴⁵Within the present model, we only describe the inertial range of turbulence and the transition towards sub-proton scales. Although the investigation of sub-proton scale turbulence is successfully described in terms of hybrid models,^{33,39} the description of electron scale turbulence would require a full Vlasov description.
- ⁴⁶A. Retinò, D. Sundkvist, A. Vaivads, F. Mozer, M. André, and C. J. Owen, *Nat. Phys.* **3**, 235 (2007).
- ⁴⁷K. T. Osman, W. H. Matthaeus, A. Greco, and S. Servidio, *Astrophys. J. Lett.* **727**, L11 (2011).
- ⁴⁸H. Karimabadi, V. Roytershteyn, M. Wan, W. H. Matthaeus, W. Daughton, P. Wu, M. Shay, B. Loring, J. Borovsky, E. Leonardis, S. C. Chapman, and T. K. M. Nakamura, *Phys. Plasmas* **20**, 012303 (2013).
- ⁴⁹F. M. Drake, M. Swisdak, C. Cattell, M. A. Shay, B. N. Rogers, and A. Zeile, *Science* **299**, 873 (2003).
- ⁵⁰J. F. Drake, M. Opher, M. Swisdak, and J. N. Chamoun, *Astrophys. J.* **709**, 963 (2010); e-print [arXiv:0911.3098](https://arxiv.org/abs/0911.3098).
- ⁵¹M. Swisdak, *Geophys. Res. Lett.* **43**, 43, <https://doi.org/10.1002/2015GL066980> (2016).

- ⁵²O. Pezzi, T. N. Parashar, S. Servidio, F. Valentini, C. L. Vásconez, Y. Yang, F. Malara, W. H. Matthaeus, and P. Veltri, *J. Plasma Phys.* **83**, 705830108 (2017).
- ⁵³H. Grad, *Commun. Pure Appl. Math.* **2**, 331 (1949).
- ⁵⁴T. Armstrong and D. Montgomery, *J. Plasma Phys.* **1**, 425 (1967).
- ⁵⁵J. W. Schumer and J. P. Holloway, *J. Comput. Phys.* **144**, 626 (1998).
- ⁵⁶Z. Yin, *J. Comput. Phys.* **258**, 371 (2014).
- ⁵⁷G. Knorr, *Plasma Phys.* **19**, 529 (1977).
- ⁵⁸C. F. Kennel and H. Petschek, *J. Geophys. Res.* **71**, 1, <https://doi.org/10.1029/JZ071i001p00001> (1966).
- ⁵⁹J. V. Shebalin, W. H. Matthaeus, and D. Montgomery, *J. Plasma Phys.* **29**, 525 (1983).
- ⁶⁰J. A. Araneda, E. Marsch, and F. Adolfo, *Phys. Rev. Lett.* **100**, 125003 (2008).
- ⁶¹F. Valentini, P. Veltri, F. Califano, and A. Mangeney, *Phys. Rev. Lett.* **101**, 025006 (2008).
- ⁶²S. D. Bale, J. C. Kasper, G. G. Howes, E. Quataert, C. Salem, and D. Sundkvist, *Phys. Rev. Lett.* **103**, 211101 (2009).
- ⁶³Y. Nariyuki, T. Hada, and K. Tsubouchi, *J. Geophys. Res.* **114**, A07102, <https://doi.org/10.1029/2009JA014178> (2009).
- ⁶⁴L. Matteini, S. Landi, M. Velli, and P. Hellinger, *J. Geophys. Res.* **115**, A09106, <https://doi.org/10.1029/2009JA014987> (2010).
- ⁶⁵N. J. Sircombe, T. D. Arber, and R. O. Dendy, *J. Phys. IV France* **133**, 277 (2006).
- ⁶⁶A. A. Schekochihin, S. C. Cowley, W. Dorland, G. W. Hammett, G. G. Howes, G. G. Plunk, E. Quataert, and T. Tatsuno, *Plasma Phys. Controlled Fusion* **50**, 124024 (2008); e-print [arXiv:0806.1069](https://arxiv.org/abs/0806.1069) [physics.plasm-ph].
- ⁶⁷D. R. Hatch, F. Jenko, V. Bratanov, and A. B. Navarro, *J. Plasma Phys.* **80**, 531–551 (2014).
- ⁶⁸J. T. Parker and P. J. Dellar, *J. Plasma Phys.* **81**, 305810203 (2015); e-print [arXiv:1407.1932](https://arxiv.org/abs/1407.1932) [physics.plasm-ph].
- ⁶⁹T. C. Li, G. G. Howes, K. G. Klein, and J. M. TenBarge, *Astrophys. J. Lett.* **832**, L24 (2016).
- ⁷⁰D. Groseelj, S. S. Cerri, A. B. Navarro, C. Willmott, D. Told, N. F. Loureiro, F. Califano, and F. Jenko, *Astrophys. J.* **847**, 28 (2017).
- ⁷¹L. Franci, S. Landi, A. Verdini, L. Matteini, and P. Hellinger, *Astrophys. J.* **853**, 26 (2018).
- ⁷²T. Adkins and A. A. Schekochihin, *J. Plasma Phys.* **84**, 905840107 (2018).
- ⁷³A. Bañón Navarro, B. Teaca, D. Told, D. Groseelj, P. Crandall, and F. Jenko, *Phys. Rev. Lett.* **117**, 245101 (2016).